

Deep Image: Scaling up Image Recognition

Ren Wu¹ Shengen Yan Yi Shan Qingqing Dang Gang Sun

ABSTRACT

We present a state-of-the-art image recognition system, Deep Image, developed using end-to-end deep learning. The key components are a custom-built supercomputer dedicated to deep learning, a highly optimized parallel algorithm using new strategies for data partitioning and communication, larger deep neural network models, novel data augmentation approaches, and usage of multi-scale high-resolution images. Our method achieves excellent results on multiple challenging computer vision benchmarks.

1. Introduction

On May 11th, 1997, IBM's Deep Blue achieved a historic victory by defeating world chess champion Gary Kasparov in a six-game match [5]. It came as a surprise to some, but with the correct algorithms, chess performance is a function of computational power [12, 24, 29]. Today, history is repeating itself: simple, scalable algorithms, given enough data and computational resources, dominate many fields, including visual object recognition [9, 27, 48], speech recognition [13, 21] and natural language processing [11, 32, 33].

Although neural networks have been studied for many decades, only recently have they come into their own, thanks to the availability of larger training data sets along with increased computation power through heterogeneous computing [10].

Because computational power is so important to progress in deep learning, we built a supercomputer designed for deep learning, along with a software stack that takes full advantage of such hardware. Using application specific hardware-software co-design, we have a highly optimized system. This system enables larger models to be trained on more data, while also reducing turnaround time, allowing us to explore ideas more rapidly.

Still, there are two shortcomings in current deep learning practices. First, while we know that bigger models offer more potential capacity, in practice, the size of model is often limited by either too little training data or too little time for running experiments, which can lead both to overfitting or underfitting. Second, the data collected is

often limited to a specific region of the potential example space. This is especially challenging very large neural networks, which are subject to overfitting.

In this work, we show how aggressive data augmentation can prevent overfitting. We use data augmentation in novel ways, much more aggressively than previous work [23, 27]. The augmented datasets are tens of thousands times larger, allowing the network to become more robust to various transformations.

Additionally, we train on multi-scale images, including high-resolution images. Most previous work [27, 51] operates on downsized images with a resolution of approximately 256x256. While using downsized images reduces computational costs without losing too much accuracy, we find that using larger images improves recognition accuracy. As we demonstrate, there are many cases where the object size is small, and downsizing simply loses too much information.

Training on higher-resolution images improves the classification accuracy. More importantly, models trained on high-resolution images complement models trained on low-resolution images. Composing models trained on different scales produces results better than any model individually.

In this paper, we detail our custom designed supercomputer for deep learning, as well as our optimized algorithms and software stack built to capitalize on this hardware. This system has enabled us to train bigger neural models, work on higher-resolution images, and use more aggressive data augmentation methods.

2. Hardware/Software Co-design

It is clear that different classes of algorithms would perform differently on different computing architectures. Graphic processors, or GPUs, often perform extremely well for compute-intensive algorithms. Early work shows that for clustering algorithms, a single GPU offers 10x more performance than top-of-the-line 8 cores workstations, even on very large datasets with more than a billion data points [50]. A more recent example shows that three GPU

¹ All the authors are with Baidu Heterogeneous Computing Group.

Ren Wu (wuren@baidu.com) is the corresponding author.

servers with 4 GPUs each, rival the same performance of a 1000 nodes (16000 cores) CPU cluster, used in the system [10].

Modern deep neural networks are mostly trained by variants of stochastic gradient decent algorithms (SGD). As SGDs contain high arithmetic density, GPUs are excellent for this type of algorithms.

Furthermore, we would like to train very large deep neural networks without worrying about the capacity limitation of a single GPU or even a single machine, and so scaling up is a required condition. Given the properties of stochastic gradient decent algorithms, it is desired to have very high bandwidth and ultra low latency interconnects to minimize the communication costs, which is needed for the distributed version of the algorithm.

The result is the custom-built supercomputer, which we call Minwa. It is comprised of 36 server nodes, each with 2 six-core Intel Xeon E5-2620 processors. Each sever contains 4 Nvidia Tesla K40m GPUs and one FDR InfiniBand (56Gb/s) which is a high-performance low-latency interconnection and supports RDMA. The peak single precision floating point performance of each GPU is 4.29TFlops and each GPU has 12GB of memory. Thanks to the GPUDirect RDMA, the InfiniBand network interface can access the remote GPU memory without involvement from the CPU. All the server nodes are connected to the InfiniBand switch. The system runs Linux with CUDA 6.0 and MPI MVAPICH2, which also enables GPUDirect RDMA.

In total, Minwa has 6.9TB host memory, 1.7TB device memory, and about 0.6PFlops theoretical single precision peak performance.

3. Optimization

Our goal is to push for extreme performance from both hardware and software for given tasks. In modern deep convolutional neural networks, convolutional layers account for most of the computation and fully-connected layers account for most of the parameters. We implement two parallelism strategies for our parallel deep neural network framework, namely model-data parallelism and data parallelism. Similar strategies have been proposed in the previous work [28, 50]. However, the previous work mainly focuses on a single server with multiple GPUs or small GPU clusters, so it's hard to extend directly to a large GPU cluster because of the communication bottlenecks. In our work, we focus on optimizing parallel strategies, minimizing data transfers and overlapping the computation and communications. This is needed for approaching the peak performance for the large supercomputers like Minwa.

3.1 Data Parallelism

When all the parameters can be stored in the memory of one GPU, we exploit data parallelism at all layers. In this case, each GPU is responsible for 1/N mini-batch of input images and all GPUs work together on the same mini-batch. In one forward-backward pass, the parameters and gradients of all layers are copied on every GPU. All GPUs compute gradients based on local training data and a local copy of weights. They then exchange gradients and update the local copy of weights.

Two strategies have helped us to achieve better parallelism. The first one is the *'butterfly synchronization'* strategy, in which all gradients are partitioned into K parts and each GPU is responsible for its own part. At the end of gradient computation, GPU k receives the k-th part from all other GPUs, accumulates there and then broadcasts the results back to all GPUs.

Another is the *'lazy update'* strategy. Once the gradients are generated in the backward pass, each GPU sends its generated gradient to the corresponding GPUs in an asynchronous way. This transfer does not need to be synchronized until its corresponding weight parameters need to be used, which only occurs later at the forward pass. This maximizes the overlapping between computation and communication.

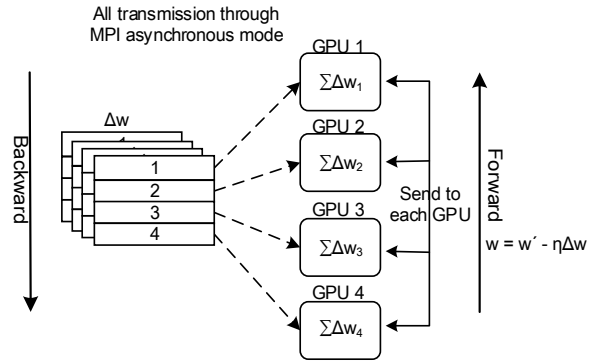


Figure 1: Example of communication strategies among 4 GPUs.

Figure 1 shows an example of the transmission on four GPUs. Theoretically, the communication overhead of our data parallel strategy only depends on the size of the model and is independent of the number of GPUs. We also use device memory to cache the training data if there is free memory space on the device after the model is loaded.

3.2 Model-Data Parallelism

While data parallelism works well for the smaller models. It does not work if the model size cannot be fit into the memory of a single GPU. Model-data parallelism is used to address this problem. Here, data parallelism is still used at convolutional layers but fully-connected layers are instead partitioned and distributed to multiple GPUs. This works

because convolutional layers have fewer parameters but more computation.

The parameters at convolutional layers are copied on every GPU and all images within one mini-batch are partitioned and assigned to all GPUs, just as we described in section 3.1. The parameters at fully-connected layers, however, are evenly divided amongst all GPUs. All GPUs then work together to calculate the fully-connected layers and synchronize when necessary. This is similar to the approach presented in [28], even though we are doing it in a scaled up fashion.

3.3 Scaling Efficiency

We tested the scaling efficiency by training a model for an image classification task. The network has 8 convolutional layers and 3 fully-connected layers followed by a 1000-way softmax. Measured by the epoch time, the scalability efficiency and the speedup of going through images are shown in Figure 2. For the convenience of observing the scalability of different parallel strategies, we fixed the number of images processed by each GPU to 64 (slices = 64). The time taken for hybrid parallelism and data parallelism with different numbers of GPUs is shown in Figure 2(a). The data parallelism performs better when the involved GPU number is larger than 16. This is because

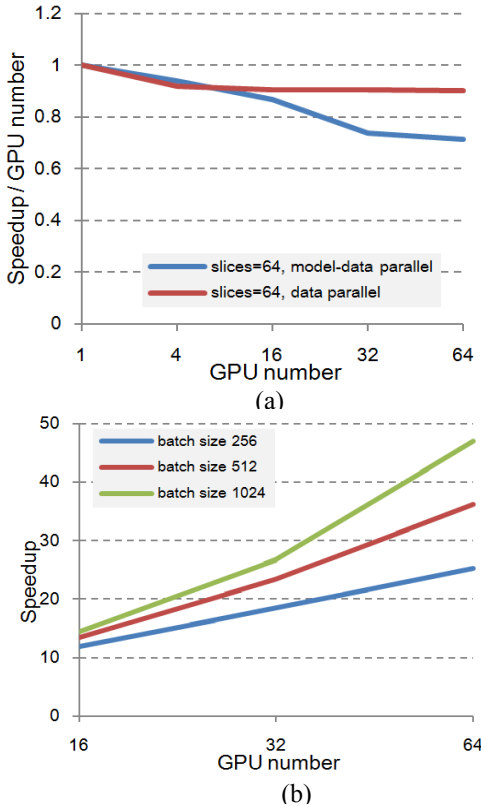


Figure 2: (a): The scalability of different parallel approaches. (b): The speedup of going through images.

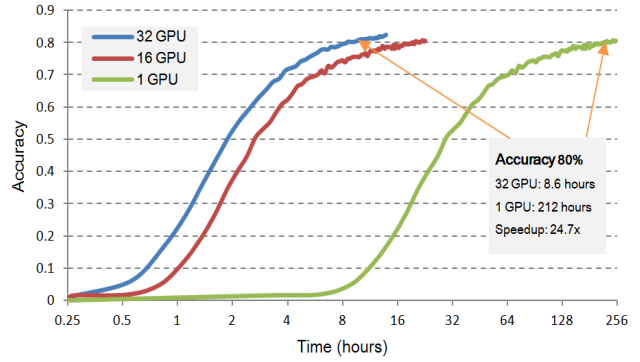


Figure 3: Validation set accuracy for different numbers of GPUs.

communication overhead of the data parallel strategy is constant when the size of model is fixed. The speedup is larger with larger batch size as shown in the Figure 2(b). Compared with a single GPU, a 47x speedup of going through images is achieved by using 64 GPUs with a mini-batch size of 1024. As the number of GPUs increases, the total device memory is also increasing, and more data can be cached on the device memory. This is helpful for improving parallel efficiency.

The ultimate test for a parallel algorithm is the convergence time, that is, the wall clock time needed for the network to reach a certain accuracy level. Figure 3 compares the time needed for the network to reach 80% accuracy using various numbers of GPUs. Note that a 24.7x speedup is obtained by using 32 GPUs.

4. Training Data

4.1 Data Augmentation

The phrase “the more you see, the more you know” is true for humans as well as neural networks, especially for modern deep neural networks. We are now capable of building very large deep neural networks up to hundreds of billions parameters thanks to dedicated supercomputers such as Minwa. The available training data is simply not sufficient to train a network of this size. Additionally, the examples collected are often just in a form of ‘good’ data – or a rather small and heavily biased subset of the possible space. It is desired to show the network with more data with broad coverage.

The authors of this paper believe that data augmentation is fundamentally important for improving the performance of the networks. We would like the network to learn the important features that are invariant for the object classes, rather than the artifact of the training images. We have explored many different ways of doing augmentation, some of which are discussed in this section.

It is clear that an object would not change its class if ambient lighting changes, or if the observer is replaced by

another. More specifically, this is to say that the neural network model should be less sensitive to colors that are driven by the illuminants of the scene, or the optical systems from various observers. This observation has led us to focus on some of the key augmentations, such as color casting, vignetting, and lens distortion, as shown in the Figure 4.

Different from the color shifting in [27], we perform color casting to alter the intensities of the RGB channels in training images. Specifically, for each image, we generate three Boolean values to determine if the R, G and B channels should be altered, respectively. If one channel should be altered, we add a random integer ranging from -20 to +20 to that channel.

Vignetting means making the periphery of an image dark compared to the image center. In our implementation, there are two randomly changeable variables for a vignette effect. The first is the area to add the effect. The second is how much brightness is reduced.

Lens distortion is a deviation from rectilinear projection caused by the lens of camera. The type of distortion and the degree of distortion are randomly changeable. The horizontal and vertical stretching of images can also be viewed as special kind of lens distortion.

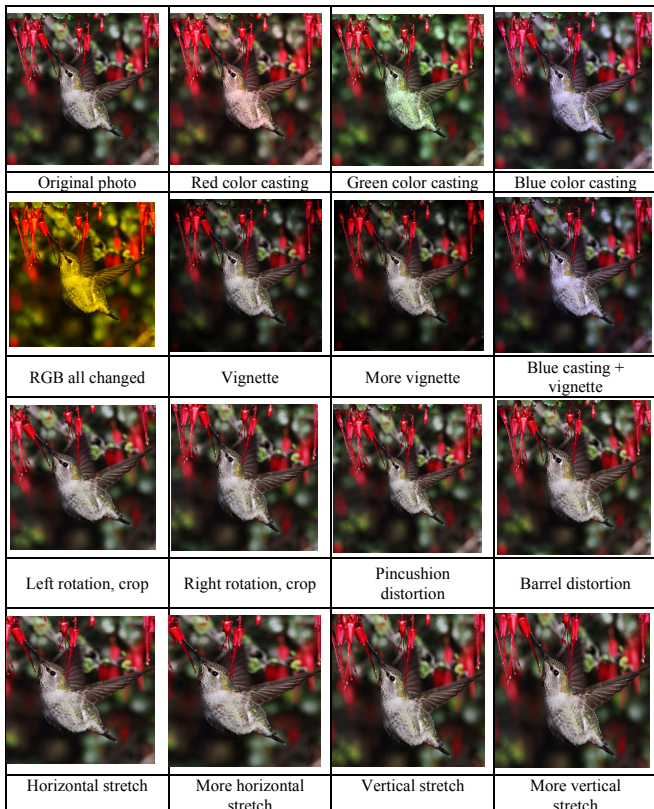


Figure 4: Effects of data augmentation.

Table 1: The number of possible changes for different augmentation ways.

Augmentation	The number of possible changes
Color casting	68920
Vignetting	1960
Lens distortion	260
Rotation	20
Flipping	2
Cropping	82944(crop size is 224x224, input image size is 512x512)

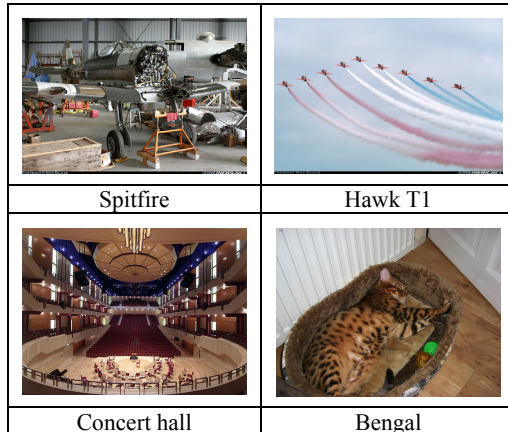


Figure 5: Some hard cases addressed by adding our data augmentation.

We also adopt some augmentations that were proposed by the previous work, such as flipping and cropping [23, 27]. To ensure that the whole augmented image feeds into the training net, all the augmentations are performed on the cropped image (except cropping).


An interesting fact worth pointing out is that both professional photographers and amateurs often use color casting and vignetting to add an artistic touch to their work. In fact, most filters offered by popular apps like Instagram are no more than various combinations of the two.

As shown in Table 1, by using different augmentation approaches, the number of training examples explodes and poses a greater challenge in terms of computational resources. However, the resulting model has better accuracy which recoups the cost as evidenced in Figure 5.

4.2 Multi-scale Training

We also notice that multi-scale training with high-resolution images works better than single-scale training, especially for recognizing small objects.

Previous work [27, 51] usually downsizes the images to a fixed resolution, such as 256x256, and then randomly crops out slightly smaller areas, such as 224x224, and uses those crops for training. While this method reduces computational costs and the multiple convolutional layers can still capture the multi-scale statistics, the down



Low-resolution model		
Rank	Score	Class
01	0.1869	Hooded Oriole
02	0.1841	Scott Oriole
03	0.1829	Blue winged Warbler
04	0.0888	Orange crowned Warbler
05	0.0759	Cardinal
06	0.0693	Rufous Hummingbird
07	0.0621	Orchard Oriole
08	0.0297	Summer Tanager

High-resolution model		
Rank	Score	Class
01	0.4970	Orchard Oriole
02	0.1185	Hooded Oriole
03	0.1042	Scott Oriole
04	0.0691	Baltimore Oriole
05	0.0622	Rufous Hummingbird
06	0.0317	Blue winged Warbler
07	0.0235	Anna Hummingbird
08	0.0225	Prairie Warbler

Figure 6: Top-8 classification results comparison between the models trained by low-resolution and high-resolution images.

sampling may disturb the details of small objects, which are important features to distinguish between different classes. If higher-resolution images such as 512x512 are used, there will be more details captured by each 224x224 crop. The model may learn more from such crops. Different from the work [45, 46] that uses scale-jittering method, we have trained separate models at different scales, including high-resolution ones (such as 512x512), and combined them by averaging softmax class posteriors.

As shown in Figure 6, the orchard oriole is small and only occupies a small portion of the image. If a model trained by low-resolution images is used, the true class is not the top-1 prediction, even out of the top-5 predictions. A high-resolution training will capture more features of orchard oriole and recognize the image in the first place. Figure 7 has more examples where a higher-resolution model gives the correct top-1 answer while the lower-resolution one fails.

On the other hand, the small crop from a high-resolution image may not contain any object that will mislead the model by giving a label of the whole image. So, a model trained by crops from low-resolution images is also necessary.

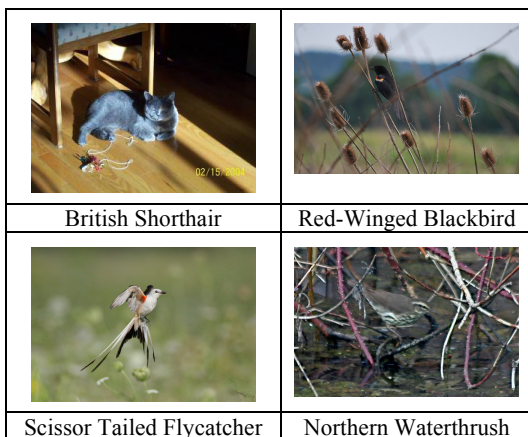


Figure 7: Some hard cases addressed by using higher-resolution images for training.

For some datasets, we have trained several models with the images of different scales and they are complementary. For example, two models pre-trained using ILSVRC [41] training images and fine-tuned using CUB-200-2011 dataset [47], at the resolution of 256x256 and 512x512 respectively, could give a top-1 accuracy rate of 83.7% and 81.6% for the test set, but the fused model by simple averaging gives an error rate of 84.9% - an even better result than each individual model.

5. Experiments

We test our system's performance on several popular computer vision benchmarks: CUB-200-2011 [47], Oxford 102 Flowers [35], Oxford-IIIT Pets [37], FGVC-Aircraft [31], MIT indoor scene [39], and ILSVRC. The first four datasets are fine-grained recognition. The fifth is for the indoor scene recognition. And the last dataset is for generic classification. Provided training and test data split is used and standard evaluation methods are followed. We report our results in the following sections.

5.1 Models and Training Details

We use two kinds of deep convolutional neural network models, similar to VGG's model [45], but most of them are larger. Figure 8 shows the two most used configurations. For 16 weight layers model, there are 13 convolutional layers and 3 fully-connected layers. For 19 weight layers model, there are 16 convolutional layers and 3 fully-connected layers. The number of output channels of each weight layer is shown in the figure and the kernel sizes of all convolutional layers are 3x3. A ReLU activation function is applied after each weight layer except the last fully-connected layer. A Dropout layer is equipped after the first two fully-connected layers and the drop out ratio is 50%. As shown in the figure, the whole network is divided into several parts by the max-pooling layer. The kernel sizes of all max-pooling layers are 2x2, and the stride sizes are 2. Various models are trained with various numbers of the kernels/parameters at convolutional layers and fully-connected layers, using different image scales (from 256x256 to 512x512) and data augmentation methods.

All the models are trained using standard training techniques and mostly default hyper-parameters [22, 25, 45, 46]. A learning rate of 0.01 is selected at the beginning and then divided by ten when the accuracy stops increasing. The input images are first resized to different resolutions for different models respectively. Then the images are augmented and randomly cropped into 224x224 patches for training.

Inspired by [43], a transformed network with only convolutional layers is used to test images and the class scores from the feature map of the last layer are averaged to attain the final score. We also tested single images at multiple scales and combined the results, which will cover

Oxford 102 Flowers

Oxford 102 flowers dataset [35] consists of 102 different categories of flowers with 8,189 images, which vary in scale, resolution, lighting clutter, quality, etc. Distinguishing features in flowers are the color, shape, patterns on the petal etc. The dataset is divided into a training set (6,149 images), a validation set (1,020 images) and a test set (1,020 images). The best result published so far [44] was heavily reliant on part model. Their best part selection scheme achieves 95.34% mean accuracy using VGG 19-layer model. The best result without part information is 93.07% [44].

We fine-tune all layers of our 19-layer model using training set without segmentation images, which are also provided by Oxford flowers dataset. Our single model with multi-scale testing achieves a state-of-the-art result with 98.73% accuracy. In fact, by treating the model as the feature extractor out-of-shelf and only fine-tuning the last softmax layer, we can achieve accuracy of 96.1%, still better than best published result of 95.34%.

Table 3. Species categorization results on Oxford flowers

Method	Accuracy(%)
Angelova et al. [1]	80.66
Murray et al. [34]	84.60
Razavian et al. [40]	86.80
Azizpour et al. [2]	91.30
No parts (AlexNet) [44]	90.35
Const. (AlexNet) [44]	91.74
No parts (VGG19) [44]	93.07
Const. (VGG19) [44]	95.34
Ours w/o seg	98.73

Oxford-IIIT Pets

The Oxford- IIIT Pets dataset [37] is created by Visual Geometry Group (VGG). The dataset contains 37 classes, 7,349 images (each class with roughly 200 images). The best result on this dataset is the work by paper [44]. They fine-tuned the VGG 19 layers model together with the unsupervised part model and achieved a 91.6% mean accuracy on 37 classes. They also provided the result without using part model, in which an 88.76% mean accuracy on 37 classes is achieved.

Table 4. Species categorization results on Oxford-IIIT pets

Method	Accuracy(%)
Bo et al. [42]	53.40
Angelova et al. [1]	54.30
Murray et al. [34]	56.80
Azizpour et al. [2]	88.10
No parts (AlexNet) [44]	78.55
Const. (AlexNet) [44]	85.20
No parts (VGG19) [44]	88.76
Const. (VGG19) [44]	91.60
Ours	93.10

Different from adopting the part model in paper [44], we only use the classification model. We simply fine-tune the last three fully-connected layers of our best single model. The same as paper [44], the training and evaluation process follow the protocol of paper [37]. The learning rate starts from 0.001 and decreased to 0.0001. Together with our data augmentation techniques, 93.1% mean accuracy is achieved with the multi-scale testing. Compared with the previous result without part model, our approach improves the mean accuracy by 4.34%.

FGVC-Aircraft

The FGVC-aircraft dataset [31] consists of 10,000 images of 100 aircraft variants, which is a part of the fine-grained recognition challenge FGComp 2013. The method in previous work [20] is an ensemble approach based on a heavily engineered version of FV-SIFT. They achieve mean per-class accuracy of 80.74% when using the provided bounding boxes information during the training stage. When using bounding boxes information at both the training and testing stage, they achieve 81.46% mean accuracy on this dataset. Another work [30] achieves mean per-class accuracy of 79.4% by using bilinear CNN model. One network is used to model “where” parts are in an image and another is used to model “what” the parts look like. The outputs of the two networks are combined bilinearly.

We use the same data split strategy as paper [20] on this dataset. By fine-tuning all layers of our 19-layer model with our data augmentation approaches, we improve the mean per-class accuracy to 85.17%, setting the new record without using any bounding box information.

Table 5. Species categorization results on aircraft variant

Method	Accuracy(%)
B-CNN(M,M), w/ ft [30]	73.5
B-CNN(D,M), w/ ft [30]	79.4
Philippe et al. track2 [20]	80.7
Philippe et al. track1 [20]	81.5
Ours	85.2

5.3 Scene Recognition

Indoor scene recognition is another challenging open problem in vision, namely place categorization. The location of meaningful regions and objects varies drastically within each category. Some indoor scenes can be well characterized by global spatial properties, while others are better characterized by the objects they contain. So this kind of scene categorization requires a model that can exploit both local and global discriminative information and in general it is a very hard problem for computer vision.

MIT indoor scenes dataset [39] contains 67 indoor scenes covering a wide range of domains including: leisure, working places, home, stores and public space categories.

It consists of 15,620 images, 80 images of each class for training and 20 images for testing. The best result in published work [8] uses a D-CNN descriptor, which is a texture descriptor based on the Fisher Vector (FV), related to the method [19]. The features are extracted using VGG 19 layer model and then a SVM classifier is used. This is the best result on MIT Indoor scene with accuracy of 81.1%.

In our experiments, we fine-tune the last three FC layers of our 19-layer pre-trained model with 5,360 provided training images without using any annotation information. Our aggressive data augmentation methods are used here again just to show more examples to the model. We achieve accuracy of 82.4% using multi-scale testing.

Table 6. Accuracy comparison of different methods on MIT-67 indoor scenes

Method	Accuracy(%)
IFV [26]	60.8
MLrep [15]	64.0
CNN-SVM [40]	58.4
CNNaug-SVM [40]	69.0
CNN(AlexConvNet)+multiscale pooling [40]	68.9
MOP-CNN [19]	68.9
D-CNN-VD [8]	81.1
Ours	82.4

5.4 Generic Classification

Note: Recently the ILSVRC organizers contacted the Heterogeneous Computing team to inform us that we exceeded the allowable number of weekly submissions to the ImageNet servers (over 200 submissions during the lifespan of our project). We apologize for this mistake, and have put processes into place to ensure it doesn't happen again. We are working with the ILSVRC organizers to review the results and will continue to provide updates to this paper as our understanding of the results improves. We are staunch supporters of fairness and transparency in the ImageNet Challenge and are committed to the integrity of the scientific process.

We have also tested our system on the ImageNet Large-Scale Visual Recognition Challenge (ILSVRC), a popular dataset for generic object classification. Only the provided data was used for training. Taking advantage of data augmentation and random crops from high-resolution training images, we were able to reduce the risk of overfitting, despite our training a relatively large model.

We trained six models with different configurations. These models are ensembled via simple averaging of their

softmax class posteriors. The resulting model achieved a top-5 error rate of 4.58%, indicating that this approach is also promising for this benchmark.

5.5 Robustness

The results reported in this paper were achieved using substantially the same framework based on deep neural networks and end-to-end training, with little or no extra annotation, information and other computer vision algorithms.

In addition, our system is also robust in real world scenarios, thanks to the aggressive data augmentation and the high-resolution images used in our training. Figure 9 shows some of the examples. The first row is the original image from various datasets listed above, others are captured by cellphone under different conditions. Our system recognizes these images correctly despite extreme transformation.

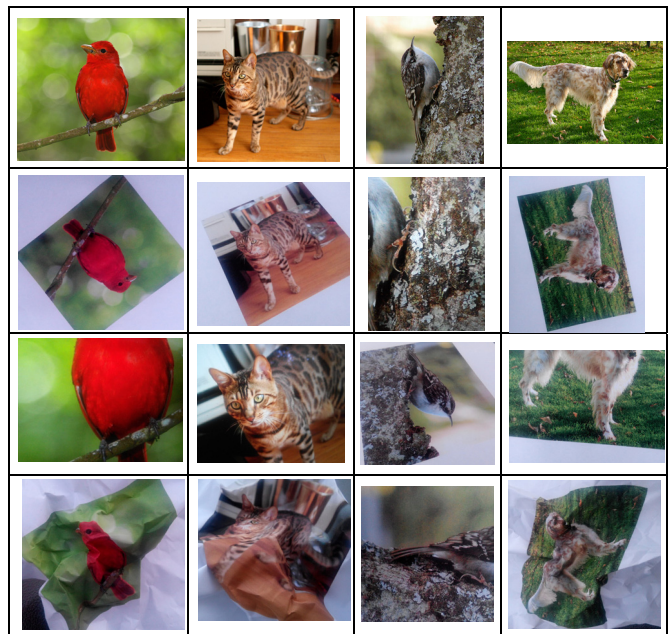


Figure 9: Experiments to test robustness.

6. Related Work

With the development of deep learning, it becomes possible to recognize and classify visual objects end-to-end without needing to create multi-stage pipelines of extracted features and discriminative classifiers. Due to the huge amount of computation, a lot of efforts have been made to build a distributed system to scale the network to very large models. Dean et al. developed DistBelief [14] to train a deep network with billions of parameters using tens of thousands of CPU cores. Within this framework, they developed asynchronous stochastic gradient descent procedure. Coates et al. built a GPU cluster with high speed interconnects, and used it to train a locally-connected

neural network [10]. Similar to this work but at a much smaller scale is the work of Paine et al. [36], in which an asynchronous SGD algorithm based on a GPU cluster was implemented. Project Adam [7] is another distributed system built by Microsoft. They trained a large network for ImageNet 22K category object classification task through asynchrony system with 62 machines in ten days and achieved top-1 accuracy of 29.8%. They did not report their result for the 1k classification challenge and so it is hard to compare this work to others. In the work [28] and [50], the authors also employed data and model parallelism or hybrid parallelization. Their systems are not scaled up and are limited to a single server with multiple GPUs.

One of the challenging problems in computer vision is the fine-grained classification task aims at the discrimination at sub-ordinate levels, such as different types of birds and flowers, which is different from generic classification. Much work has been devoted on the learning of object parts that benefits from the alignment and segmentation [1, 8, 6, 18]. Current state-of-the-art results for bird species recognition have been achieved in [4], where the strength of deep feature learning is integrated with part modeling. Most of these methods need extra bounding box and part annotations for training. However, these requirements limit their scalability to the visual domains where the acquirement of part annotations is intractable. Recently, the method proposed in [44] obtains a competitive result in fine-grained recognition without part annotations, while it still uses an unsupervised part model. Unlike the aforementioned work, we tackle the problem with our generic system, trained by end-to-end deep learning, using minimal, or not using at all, extra knowledge (i.e., part annotations or bounding box) or part modeling. Nevertheless, we still set new state-of-the-art results on four challenging fine-grained classification datasets benefiting from scalable computation (i.e., aggressive data augmentation techniques and large neural networks).

Indoor scene classification is another challenging task in computer vision. Different from outdoor scenes, it has large variability across different samples within each category. The work [39] created a dataset of 67 indoor scenes categories, which was used by many researchers [8, 15, 19, 26, 40]. Quattoni et al. propose a scene model which uses image prototypes to define a mapping between images and scene labels. Juneja et al. [26] present an automatic discovery of distinctive parts for an object or scene class and show that the method can learn parts more informatively on the MIT Scene 67 benchmark. This is a weakly supervised method. They also show that a well constructed improved Fisher Vector model works well on this scene dataset. Doersch et al. pose a mid-level visual element discovery as discriminative mode seeking and evaluate this method on the task of scene recognition, outperforming the work [15]. Different from these work,

several work uses CNN to address the indoor scene recognition. The published work [40] using a CNN off-the-shelf representation with linear SVMs training improves the baselines. The scheme presented by Gong et al. extracts CNN activations for local patches at multiple scale levels, and then performs orderless VLAD encoding. Finally, they train a linear SVMs classifier. The previous best result [8] is obtained by Fisher Vector pooling of a deep CNN filter bank. In contrast, we only fine-tune our pre-trained model with our aggressive data augmentation methods and use the softmax layer as the classifier layer. We set the new state-of-the-art mean accuracy on MIT Scene 67 dataset.

7. Conclusion

We have built a large supercomputer dedicated to training deep neural networks. By training a large model using high-resolution images and seeing a large number of examples, our system has achieved excellent results on multiple benchmarks.

This work is driven by tremendous computational power, and can also be described as a “brute force” approach. It is possible that other approaches will yield the same results with less demand on the computational side. The authors of this paper argue that with more human effort being applied, it is indeed possible to see such results. However, human effort is precisely what we want to avoid.

8. Acknowledgments

The Minwa project started in October 2013, after an interesting discussion on a high-speed train from Beijing to Suzhou. Many thanks to the Baidu SYS group for their help with hosting the Minwa supercomputer and to Zhiqian Wang for helping with benchmarking the hardware components.

9. References

- [1] A. Angelova and S. Zhu, Efficient object detection and segmentation for fine-grained recognition. *In CVPR, 2013*.
- [2] H. Azizpour, A. S. Razavian, J. Sullivan, A. Maki, and S. Carlsson. From generic to specific deep representations for visual recognition. *CoRR, abs/1406.5774, 2014*.
- [3] T. Berg and P. N. Belhumeur. Poof: Part-based one-vs.-one features for fine-grained categorization, face verification, and attribute estimation. *In Computer Vision and Pattern Recognition (CVPR), pages 955–962. IEEE, 2013*.
- [4] S. Branson, G. Van Horn, P. Perona, and S. Belongie. Improved bird species recognition using pose normalized deep convolutional nets. *In British Machine Vision Conference, 2014*.
- [5] M. Campbell, A.J. Hoane, and F. Hsu. Deep Blue. *Artificial Intelligence 134, pages 57–59. 2002*.

- [6] Y. Chai, V. Lempitsky, and A. Zisserman. Symbiotic segmentation and part localization for fine-grained categorization. *In International Conference on Computer Vision (ICCV)*, pages 321–328. IEEE, 2013.
- [7] T. Chilimbi, Y. Suzue, J. Apacible, and K. Kalyanaraman. Project Adam: Building an efficient and scalable deep learning training system. *To appear in the 11th USENIX Symposium on Operating Systems Design and Implementation '14 (OSDI)*, Oct. 2014.
- [8] M. Cimpoi, S. Maji, A. Vedaldi, Deep convolutional filter banks for texture recognition and segmentation, *arXiv:1411.6836*, 2014.
- [9] D.C. Ciresan, U. Meier, L.M. Gambardella, and J. Schmidhuber. Deep big simple neural nets excel on handwritten digit recognition. *CoRR*, 2010.
- [10] A. Coates, B. Huval, T. Wang, D.J. Wu, A.Y. Ng, and B. Catanzaro. Deep learning with COTS HPC. *In ICML*, 2013.
- [11] R. Collobert and J. Weston. A unified architecture for natural language processing: Deep neural networks with multitask learning. *In ICML*, 2008.
- [12] J. Condon and K. Thompson. Belle chess hardware. *Advances in Computer Chess 3*, 1982.
- [13] G. Dahl, D. Yu, L. Deng, and A. Acero. Context-dependent pre-trained deep neural networks for large vocabulary speech recognition. *IEEE Transactions on Audio, Speech, and Language Processing*, 2012.
- [14] J. Dean, G.S. Corrado, R. Monga, K. Chen, M. Devin, Q.V. Le, M.Z. Mao, M.A. Ranzato, A. Senior, P. Tucker, K. Yang, and A.Y. Ng. Large scale distributed deep networks. *In NIPS*. 2012.
- [15] C. Doersch, A. Gupta, and A. A. Efros. Mid-level visual element discovery as discriminative mode seeking. *In NIPS*, 2013.
- [16] J. Donahue, Y. Jia, O. Vinyals, J. Hoffman, N. Zhang, E. Tzeng, and T. Darrell. Decaf: A deep convolutional activation feature for generic visual recognition. *arXiv:1310.1531*, 2013.
- [17] E. Gavves, B. Fernando, C. G. Snoek, A. W. Smeulders, and T. Tuytelaars. Local alignments for fine-grained categorization. *International Journal of Computer Vision*, pages 1–22, 2014.
- [18] R. Girshick, J. Donahue, T. Darrell, and J. Malik. Rich feature hierarchies for accurate object detection and semantic segmentation. *In Computer Vision and Pattern Recognition*, 2014.
- [19] Y. Gong, L. Wang, R. Guo, and S. Lazebnik. Multi-scale orderless pooling of deep convolutional activation features. *In Proc. ECCV*, 2014.
- [20] P.-H. Gosselin, N. Murray, H. J' egou, and F. Perronnin. Revisiting the fisher vector for fine-grained classification. *Pattern Recognition Letters*, 49:92–98, 2014.
- [21] A. Hannun, C. Case, J. Casper, B. Catanzaro, G. Diamos, E. Elsen, R. Prenger, S. Satheesh, S. Sengupta, A. Coates, and A.Y. Ng. DeepSpeech: Scaling up end-to-end speech recognition. *arXiv:1412.5567*, 2014.
- [22] K. He, X. Zhang, S. Ren and J. Sun, Delving Deep into Rectifiers: Surpassing Human-Level Performance on ImageNet Classification. *arXiv:1502.01852*, 2015.
- [23] A.G. Howard, Some improvements on deep convolutional neural network based image classification. *CoRR*, *abs/1312.5402*, 2013.
- [24] R. Hyatt, A. Gower, and H. Nelson. Cray Blitz. *Computers, Chess, and Cognition*, pages 111-130, 1990.
- [25] S. Ioffe, and C. Szegedy, Batch Normalization: Accelerating Deep Network Training by Reducing Internal Covariate Shift. *arXiv:1502.03167*, 2015.
- [26] M. Juneja, A. Vedaldi, C. V. Jawahar, and A. Zisserman. Blocks that shout: Distinctive parts for scene classification. *In CVPR*, 2013.
- [27] A. Krizhevsky, I. Sutskever, and G.E. Hinton. Imagenet classification with deep convolutional neural networks. *In NIPS*, volume 1, page 4, 2012.
- [28] A. Krizhevsky. One weird trick for parallelizing convolutional neural networks. *arXiv:1404.5997*, 2014.
- [29] B.C. Kuszmaul. The StarTech massively parallel chess program. *Journal of the International Computer Chess Association*, 18(1), March 1995.
- [30] T. Lin, A.R. Chowdhury, S. Maji, Bilinear CNN Models for Fine-grained Visual Recognition, *arXiv:1504.07889* 2015.
- [31] S. Maji, E. Rahtu, J. Kannala, M. Blaschko, and A. Vedaldi. Fine-grained visual classification of aircraft. *arXiv:1306.5151*, 2013.
- [32] A. Mnih and G. Hinton. A scalable hierarchical distributed language model. *The Conference on Neural Information Processing Systems (NIPS)*, pp. 1081–1088. 2008.
- [33] A. Mnih and G. Hinton. Three new graphical models for statistical language modeling. *In ICML*. 2007.
- [34] N. Murray and F. Perronnin. Generalized max pooling. *In CVPR*, 2014.
- [35] M.-E. Nilsback and A. Zisserman. Automated flower classification over a large number of classes. *In Proceedings of the Indian Conference on Computer Vision, Graphics and Image Processing*, Dec 2008.
- [36] T. Paine, H. Jin, J.C Yang, Z. Lin, and T. Huang. GPU asynchronous stochastic gradient descent to speed up neural network training. *In ICLR*, April 2014.

- [37] O.M. Parkhi, A. Vedaldi, A. Zisserman and C.V. Jawahar, Cats and dogs. *In CVPR 2012*.
- [38] J. Pu, Y.-G. Jiang, J. Wang, and X. Xue. Which looks like which: Exploring inter-class relationships in fine-grained visual categorization. *In European Conference on Computer Vision (ECCV), pages 425–440. Springer, 2014*.
- [39] A. Quattoni and A. Torralba. Recognizing indoor scenes. *In CVPR, 2009*.
- [40] A.S. Razavian, H. Azizpour, J. Sullivan, and S. Carlsson. CNN features off-the-shelf: An astounding baseline for recognition. *In CVPRW, 2014*.
- [41] O. Russakovsky, J. Deng, H. Su, J. Krause, S. Satheesh, S. Ma, Z.H. Huang, A. Karpathy, A. Khosla, M. Bernstein, A.C. Berg, L. Fei-Fei. ImageNet large scale visual recognition challenge. *arXiv:1409.0575, 2014*.
- [42] P. Sermanet, A. Frome, and E. Real. Attention for finegrained categorization. *arXiv:1412.7054, 2014*.
- [43] P. Sermanet, D. Eigen, X. Zhang, M. Mathieu, R. Fergus, and Y. LeCun. OverFeat: Integrated recognition, localization and detection using convolutional networks. *In Proc. ICLR, 2014*.
- [44] M. Simon and E. Rodner, Neural Activation Constellations: Unsupervised Part Model Discovery with Convolutional Networks. *arXiv:1504.08289, 2015*.
- [45] K. Simonyan and A. Zisserman. Very deep convolutional networks for large-scale image recognition. *arXiv:1409.1556, 2014*.
- [46] C. Szegedy, W. Liu, Y. Jia, P. Sermanet, S. Reed, D. Anguelov, D. Erhan, V. Vanhocke, and A. Rabinovich. Going deeper with convolutions. *arXiv:1409.4842, 2014*.
- [47] C. Wah, S. Branson, P. Welinder, P. Perona, and S. Belongie. The Caltech-UCSD Birds-200-2011 Dataset. *Technical Report CNS-TR-2011-001, California Institute of Technology, 2011*.
- [48] R. Wu, B. Zhang, and M. Hsu. Clustering cillions of data points using GPUs. *In ACM UCHPC-MAW, 2009*.
- [49] T. Xiao, Y. Xu, K. Yang, J. Zhang, Y. Peng and Z. Zhang. The Application of Two-level Attention Models in Deep Convolutional Neural Network for Fine-grained Image Classification. *arXiv:1411.6447, 2014*.
- [50] O. Yadan, K. Adams, Y. Taigman, and M.A. Ranzato. Multi-gpu training of convnets. *arXiv:1312.5853, 2013*.
- [51] M.A. Zeiler and R. Fergus. Visualizing and understanding convolutional networks. *CoRR, abs/1311.2901, 2013*.
- [52] N. Zhang, J. Donahue, R. Girshick, and T. Darrell. Partbased r-cnns for fine-grained category detection. *In European Conference on Computer Vision (ECCV), pages 834–849. Springer, 2014*.
- [53] N. Zhang, R. Farrell, F. Iandola, and T. Darrell. Deformable part descriptors for fine-grained recognition and attribute prediction. *In International Conference on Computer Vision (ICCV), pages 729–736. IEEE, 2013*.